Hybrid density functional theory study of the high-pressure polymorphs of α-Fe_2O_3 hematite

Nicholas C. Wilson
CSIRO Minerals, Bayview Avenue, Clayton, Victoria 3169, Australia and Applied Physics, School of Applied Sciences, RMIT University, Melbourne 3001, Australia

Salvy P. Russo
Applied Physics, School of Applied Sciences, RMIT University, Melbourne 3001, Australia
(Received 25 July 2008; published 24 March 2009)

The relative stability with respect to pressure of four structural polymorphs of Fe_2O_3 has been studied using the B3LYP hybrid exchange density functional theory, and for each polymorph a range of charge, spin, and magnetic states were examined. It was found that the B3LYP functional computed charge, magnetic ordering, structural, and elastic properties of corundum structure Fe_2O_3 are in good agreement with experiment. Magnetic ordering was found to be important for all the polymorphs, and for each polymorph antiferromagnetic ordering was found to be lower in energy than ferromagnetic ordering. The Rh_2O_3-II structure was calculated to be metastable, with the transition pressure from the corundum structure and the pressure at which magnetic collapse of Fe^{3+} cations occur in good agreement with experiment. At high pressures the lowest-energy configuration for the orthorhombic perovskite structure was computed to occur with mixed high-spin/low-spin Fe^{3+} cations. The $CaIrO_3$-type structure was also computed to be stable with a mixed high-spin/low-spin Fe^{3+} configuration at high pressures, and is computed to be the most stable polymorph at pressures above 46 GPa at 0 K. Overall we predict a number of phase-transition pressures which have been experimentally observed and give some insight into the mechanisms underlying the structural transformations.

DOI: 10.1103/PhysRevB.79.094113 PACS number(s): 61.50.Ks, 71.15.Mb, 71.30.+h

I. INTRODUCTION

Hematite (α-Fe_2O_3) and its high-pressure polymorphs have been the subject of numerous high-pressure experimental studies.[1–10] Fe_2O_3 is an important end-member compound in geophysics being studied for the understanding of the role of ferric oxides in the composition and dynamics of the earth's mantle. Despite the numerous experiments, the structural phases that hematite transforms to under pressure have not been unambiguously defined.[1] Simulation of Fe_2O_3 is challenging, as the Fe *d* shell is partially occupied, which means for each structural polymorph there are a range of charge, spin, and magnetic states allowed. It also presents a challenge to theory, as the Fe *d* electrons are strongly correlated and the widely used local-density approximation (LDA) and generalized gradient approximation (GGA) to DFT have a strong tendency to describe wide band-gap magnetic insulators as nonmagnetic metals due to the incorrect treatment of electronic self interaction.[11]

At ambient pressure the stable polymorph of Fe_2O_3 is hematite, which has a $R\bar{3}c$ corundum structure[12] (Fig. 1). In this structure iron is octahedrally coordinated with oxygen, and experimentally is found to be trivalent with a high-spin (HS) d^5-electron configuration.[13] Below its Néel temperature of 948 K,[14] hematite is observed to be antiferromagnetic (AFM),[15] with alternating (0001) layers of spin-up and spin-down iron (giving a magnetic space group of $R\bar{3}$), and between the Néel temperature and the Morin temperature of 263 K (Ref. 16) shows a weak ferromagnetism due to a slight canting of the sublattice magnetizations.

Compression studies have proposed that under pressure Fe_2O_3 transforms to either a Rh_2O_3(II) (Refs. 4–6) (Fig. 2) or a *Pbnm* orthorhombic perovskite with the gadolinium ferrite ($GdFeO_3$) (Ref. 2) structure (Fig. 3). The uncertainty in assigning the phase to either one of these structures arises because both structures give a reasonable fit to the measured x-ray diffraction patterns.[1] However, the Rh_2O_3(II) structure has only one cation site which is octahedrally coordinated with oxygen, whereas the orthorhombic perovskite structure has two distinct cation sites, one sixfold coordinated and the other eightfold, allowing for two types of iron cation. In order to determine which structure occurs, a range of spectroscopic measurements[5,7,8,10] have been performed to establish the charge and spin state of Fe.

Mossbauer spectroscopy experiments[5] performed at room temperature on the high-pressure phase imply that only one crystallographic site exists, suggesting the Rh_2O_3(II) structure. Consistent with this, results from room-temperature Raman spectroscopy[7] were also incompatible with the $GdFeO_3$ perovskite structure. Room-temperature x-ray emission spectroscopy has been used to examine the iron spin state,[8] demonstrating that the crystallographic change was independent of the change in electron-spin state.

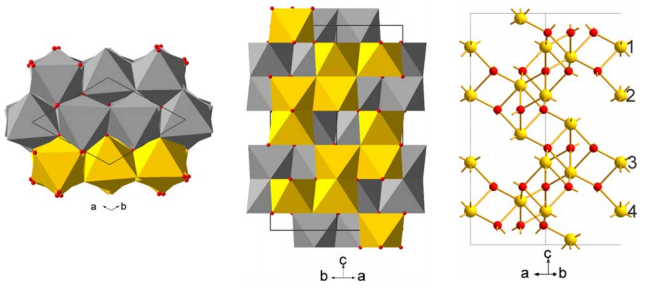

FIG. 1. (Color online) Corundum structure. Polyhedra in the front $(11\bar{2}0)$ plane highlighted in light gray (yellow online). Numbering is used to indicate magnetic ordering in the text.

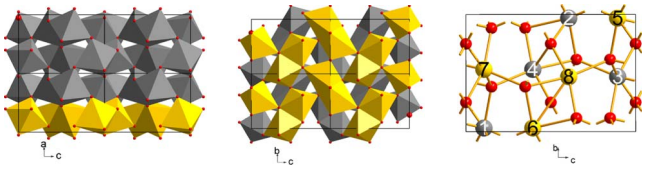

FIG. 2. (Color online) Rh_2O_3-(II) type structure. Polyhedra in the front (100) plane highlighted in light gray (yellow online). Numbering is used to indicate magnetic ordering in the text.

While room-temperature compression studies observe the phase transition at about 50–55 GPa, high-temperature experiments[1–3] performed between 800–2500 K give an estimated transition pressure when extrapolated to 300 K of 26 GPa. This discrepancy in transition pressures was explained by Ono *et al.*,[1] suggesting the 50 GPa transition could be a corundum to Rh_2O_3(II) transition, and the 26 GPa transition as a corundum to orthorhombic perovskite transition, with the corundum to perovskite transition occurring only at high temperatures due to kinetic limitations.

At pressures of about 60 GPa and temperatures greater than 1200 K, Fe_2O_3 has been observed to transform to a *Cmcm* $CaIrO_3$ structure[2,3] (Fig. 4). This structure has also been observed at high pressures in the important mantle phase of $MgSiO_3$ (Refs. 17 and 18) and also in $MgGeO_3$ (Ref. 19) and Al_2O_3.[20]

Ab initio calculations of the relative phase stability are complicated by the importance of magnetism in Fe_2O_3. Experimentally hematite is found to be antiferromagnetic, with previous DFT calculations having found the antiferromagnetic solution to be 0.776 eV per formula unit more stable than the ferromagnetic solution within the GGA,[21] and 0.98 eV (Ref. 22) per formula unit within the LDA. This stabilization energy is not small and so antiferromagnetic solutions must be considered for an accurate understanding of the high pressure phases. Two previous *ab initio* studies[6,21] have considered the effect of pressure on Fe_2O_3, however neither of these studies have considered all four polymorphs and their various magnetic states. Rollmann *et al.*[21] considered the effect of pressure only on the corundum structure, while investigating its various magnetic and electronic configurations. Rozenberg *et al.*,[6] while not examining the various magnetic configurations, considered the corundum, Rh_2O_3(II), and perovskite structures, performing both LDA and GGA calculations and predicting a corundum to Rh_2O_3(II) transition at about 20–25 GPa. While this value is in agreement with the experimental transition seen at 26 GPa, it is in disagreement with the explanation put forward by Ono *et al.*[1] that this is a corundum to perovskite transformation.

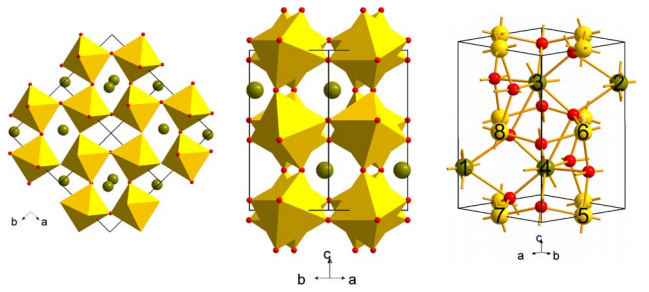

FIG. 3. (Color online) $GdFeO_3$ distorted perovskite structure. Light spheres (yellow online) represent Fe in a sixfold site, while green spheres represent Fe in the eightfold site. Numbering is used to indicate magnetic ordering in the text.

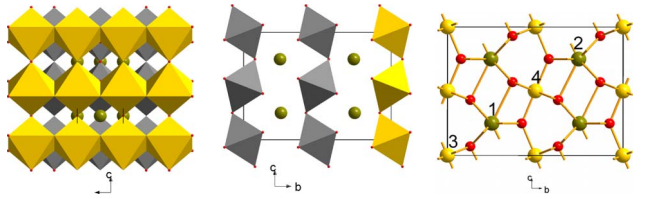

FIG. 4. (Color online) $CaIrO_3$-type structure. Polyhedra in the front (010) plane highlighted in light gray (yellow online). Numbering is used to indicate magnetic ordering in the text.

To investigate the nature of Fe_2O_3 under pressure we have performed *ab initio* calculations to predict the relative stability of the corundum, Rh_2O_3(II), *Pbmn* orthorhombic perovskite and *Cmcm* $CaIrO_3$ polymorphs of Fe_2O_3. Within each of these four polymorphs a range of ferromagnetic and antiferromagnetic solutions were examined, along with high- and low-spin (LS) Fe^{3+} states, and for the *Pbmn* and *Cmcm* structures, Fe^{2+}/Fe^{4+} charge states were also considered.

II. COMPUTATIONAL DETAILS

These calculations have been performed using the CRYSTAL03 code.[23] Treatment of electron exchange and correlation was performed using the B3LYP hybrid exchange functional.[24] This was chosen because unlike the LDA or GGA functionals, a qualitatively correct ground state is obtained for a wide range of transition-metal oxides.[11,25–30] Hybrid DFT methods have also been shown to give better results for magnetic properites[31] than LDA or GGA.

Calculations have been performed using collinear spins. The accuracy of the calculation of the bielectronic Coulomb and exchange series is dependent on the truncation of the atomic-orbital overlap integrals. The truncation of these overlap integrals are controlled by five cutoff tolerances donated as ITOL1, ITOL2, ITOL3, ITOL4, and ITOL5, which in the current study have been set to 1×10^{-7}, 1×10^{-7}, 1×10^{-7}, 1×10^{-7}, and 1×10^{-14}, respectively. The reciprocal space integration was performed by sampling the Brillouin zone using the Monkhorst-Pack scheme[32] with a shrinking factor of 8. The self-consistent field calculation was converged with a tolerance of 1×10^{-7} Ha per unit cell in total energy. The basis sets used here were developed and optimized in previous calculations of hematite Fe_2O_3.[33] The cell parameters of the Fe_2O_3 polymorphs were optimized using numerical energy gradients, while the internal coordinates were optimized using analytical energy gradients[34,35] to a tolerance on the maximum and rms forces of 0.00045 and 0.0003 Hartree/Bohr.

Calculations at finite pressures were performed by applying a hydrostatic pressure and performing a minimization of the enthalpy with respect to the cell parameters and internal coordinates, where the enthalpy (H) is given by

$$H = U + PV$$

where U is the internal energy, P the chosen pressure, and V the volume. To study the phase stability of the various elec-

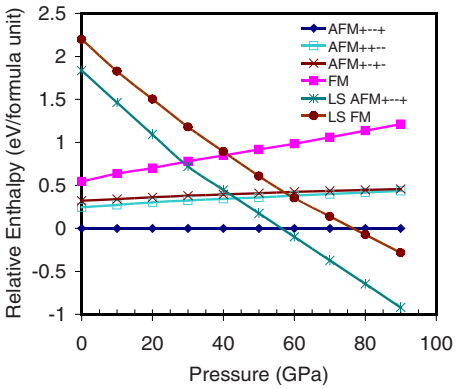

FIG. 5. (Color online) Enthalpies of the various magnetic orderings considered for the corundum structured Fe_2O_3 plotted relative to AFM+−−+ state.

tronic and structural polymorphs with respect to pressure, minimization of the enthalpy for each polymorph was performed for a set of pressures between 0 and 90 GPa.

III. RESULTS

A. Corundum structure

For the corundum structure, eight different combinations of magnetic and spin states were considered. The magnetic states are labeled from Fig. 1, where AFM+−−+ is an antiferromagnetic state with Fe atoms 1 and 4 having opposite magnetic moment to Fe atoms 2 and 3. The enthalpies of the corundum structure with various magnetic and spin configurations are plotted relative to the high-spin AFM+−−+ state in Fig. 5. At 0 GPa the high-spin Fe^{3+} AFM+−−+ state is calculated to be most stable, in agreement with experminent.[15] The projected density of states (DOS) for this state is given in Fig. 6, and shows a band gap of approximately 3 eV, which while larger than the experimental value of 2.0–2.2 eV,[36,37] is reasonable when compared to previous GGA-DFT [0.3 eV (Ref. 21)], LDA [0.51 eV,[38] 0.75 eV (Ref. 22)], Hartree-Fock (HF) [15 eV (Refs. 33 and 39)], and B3LYP [4.1 eV (Ref. 40)] band-gap predictions. The previous B3LYP calculations[40] were performed treating the core electrons with a Durand pseudopotential, while the present

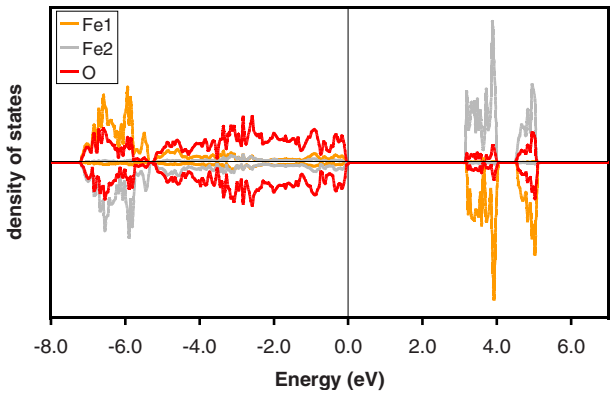

FIG. 6. (Color online) Atom projected density of electronic states near the Fermi level of AFM+−−+ corundum structure.

TABLE I. Energies (eV per formula unit) relative to the AFM +−−+ state, and a Mulliken analysis of the net atom spin for the various magnetic and spin states of hematite at 0 GPa.

	Energy (eV)	$\lvert\alpha-\beta\rvert$ Fe	$\lvert\alpha-\beta\rvert$ O
AFM+−−+	0	4.16	0.00
AFM++−−	0.245	4.21	0.11
AFM+−+−	0.322	4.21	0.00
FM	0.547	4.27	0.48
LS AFM+−−+	1.836	1.04	0.00
LS FM	2.198	1.12	0.08

calculation uses an all-electron basis set. LDA+U (Refs. 38, 41, and 42) and GGA+U (Ref. 21) can achieve the correct band gap by choosing an appropriate value for Hubbard U parameter.[43] The upper edge of the calculated valence band is dominated by O 2p states, while the lower conduction band is mainly Fe 3d in character, agreeing with experiment[13,44,45] that hematite is a charge-transfer insulator.

There have been numerous experimental determinations of the bulk modulus, giving values of 178,[46] 199,[47] 203,[48] 206,[4] 225,[49] 230,[9] 231,[46] and 258 (Ref. 6) GPa. The bulk modulus of the AFM+−−+ phase was calculated by fitting a Birch-Murnaghan equation of state[50] to an energy-volume curve generated from ten full geometry relaxations at pressures ranging from −8 to 10 GPa in 2 GPa steps. The calculated zero pressure bulk modulus is 215 GPa, with a pressure derivative $B'=3.1$, which sits within the range of experimental values. The calculated $\mathbf{c}/\mathbf{a}$ ratio of hematite decreases with increasing pressure, as is found experimentally. At 0 GPa the $\mathbf{c}/\mathbf{a}$ ratio is calculated to be 2.74 and decreases to 2.62 at 90 GPa.

Table I gives the relative stability of the various magnetic configurations of hematite at 0 GPa. The ferromagnetic solution is calculated to be 0.55 eV per formula unit less stable than the antiferromagnetic solution, a slightly lower value than the 0.78 eV per formula unit calculated within the GGA by Rollmann *et at*,[21] and lower than the value calculated by Sandratskii *et al.*,[22] within the LDA, of 0.98 eV per formula unit. The energy difference in the GGA calculations of Rollmann *et al.* are, as in the present work, calculated from relaxed geometries, while the LDA calculation of Sandratskii *et al.* used fixed geometries. While the energy differences between the ferromagnetic and antiferromagnetic solutions calculated within the B3LYP approximation are less than those calculated within the GGA and the LDA, B3LYP studies in other systems[11] would suggest that the B3LYP approximation is still overestimating these energy differences. Figure 5 shows the ferromagnetic (FM) solution is calculated to become increasingly less stable with increasing pressure, being 1.2 eV less stable than the AFM+−−+ state at 90 GPa. The AFM+−+− and AFM++−− states are also found to be more stable than the ferromagnetic solution, but not as stable as the AFM+−−+ state.

It is possible to extract approximate magnetic coupling constants from periodic calculations from the energy differences of the various magnetic solutions using an Ising

TABLE II. Structural parameters of hematite at 0 GPa for the various magnetic and spin states.

	a (Å)	c (Å)	c/a
FM	5.13	13.95	2.72
AFM++−−	5.12	13.82	2.70
AFM+−−+	5.076	13.93	2.74
AFM+−+−	5.10	13.90	2.73
LS FM	4.94	12.96	2.62
LS AFM+−−+	4.87	13.27	2.72
Expt. (AFM+−−+)	5.038	13.772	2.73

model,[51] bearing in mind the limitations of such an approach. The four types of cation-anion-cation paths are given by J_1 the Fe-O-Fe linkage through 86°, J_2 the linkage through 94°, J_3 the linkage through 120°, and J_4 the linkage through 132°. Using $S=5/2$, we obtain values of $J_2=49.8$ K, $J_4=-48.3$ K, and $J_1+3J_3=-169.2$ K. Values for the magnetic coupling constants determined from neutron scattering[52] are $J_1=6.0$ K, $J_2=1.6$ K, $J_3=-29.7$ K, and $J_4=-23.2$ K. The B3LYP result for J_4 is about twice the experimental value, which is typical for magnetic coupling constants derived from B3LYP calculations,[11,53] while the value for J_2 derived from the B3LYP calculations is significantly overestimated.

In addition to Fe^{3+} in a high-spin state, we also considered Fe^{3+} in a LS state. The ferromagnetic low-spin Fe corundum structure was computed to be 2.2 eV per formula unit higher in energy at 0 GPa than the high-spin AFM+−−+ configuration, but with increasing pressure becomes more energetically favorable, and at about 42 GPa it is more stable than the high spin ferromagnetic solution, and becomes more favorable than the high-spin antiferromagnetic solution at 75 GPa. The energy stabilization found for the high-spin state in going from a ferromagnetic to AFM+−−+ state is also found for low-spin Fe. The low-spin Fe AFM+−−+ state is calculated to be 0.36 eV per formula unit more stable than the ferromagnetic low-spin solution at 0 GPa, less than the 0.55 eV energy difference in the high-spin state. The low-spin AFM+−−+ state becomes the most stable arrangement of the corundum structure at 57 GPa.

Net spins on the Fe atom have been calculated from a Mulliken population analysis, and are presented in Table I. The high-spin solutions have a net Fe spin of about 4.2 $|e|$, slightly lower than the expected 5 $|e|$ for a high-spin d^5 solution, but consistent with the value of 4.26 $|e|$ calculated within the B3LYP approximation for high-spin Fe^{3+} in $FeTiO_3$.[29] For low-spin Fe, the Mulliken analysis gives a value of about 1 $|e|$, as expected for Fe with a low-spin d^5 configuration. Table II gives structural parameters calculated for the various spin and magnetic states of hematite. The relaxed cell parameters of the computed ground-state AFM +−−+ solution are in good agreement with experimental values, with an error of about 1%. Calculated Fe-O and Fe-Fe distances at various pressures are listed, together with experimental values taken from Ref. 6 in Table III. At 0 GPa we are in good agreement with the experimental values, and with increasing pressure there is a decrease in all of the bond lengths. At 46 GPa, we are slightly overestimating the Fe-Fe bond lengths and the face-shared Fe-O distance, while underestimating the edge shared Fe-O distance.

TABLE III. Selected interatomic distances for the hematite phase (in Å) at various pressures.

Pressure (GPa)	Fe-O (Å)	Fe-Fe (Å)
0	1.9597(F)[b]	2.953(F)
	2.142 (E)	2.998 (E)
2.9[a]	1.924(F)	2.880(F)
	2.122(E)	2.958 (E)
30	1.882(F)	2.858(F)
	2.069(E)	2.912 (E)
46[a]	1.771(F)	2.632(F)
	2.158(E)	2.841 (E)
50	1.850(F)	2.812(F)
	2.031(E)	2.873 (E)
60	1.8375(F)	2.795(F)
	2.014(E)	2.858 (E)

[a]Experimentally determined values from Ref. 6.
[b](E) denotes distances corresponding to shared edges; (F) denotes distances corresponding to shared faces.

B. Rh_2O_3(II) structure

Figure 7 shows the enthalpies of the various magnetic and spin states calculated for the Rh_2O_3(II) structure relative to the Rh_2O_3(II) high-spin AFM+−−+−−+ state, where the magnetic states are labeled from Fig. 2. In the corundum structure the most stable antiferromagnetic solution (AFM +−−+) was found to comprise of alternating (0001) layers of spin-up Fe and spin-down Fe, while for the Rh_2O_3(II) structure we find the most stable magnetic state (AFM+−−+−+−−+) having alternating spin-up and spin-down Fe in each (001) layer. The ferromagnetic solution is 0.47 eV per for-

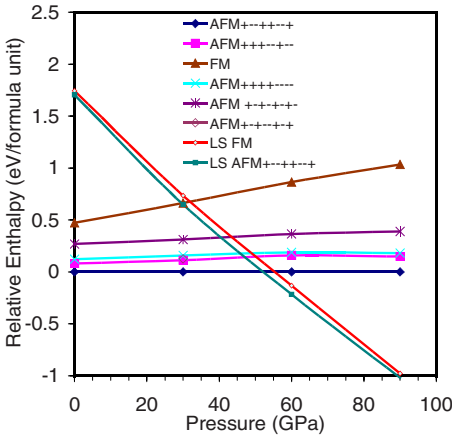

FIG. 7. (Color online) Enthalpies of the various magnetic orderings considered for the Rh_2O_3-(II) structured Fe_2O_3 plotted relative to AFM+−−+−−+ state.

TABLE IV. Energies (eV per formula unit) relative to the AFM+--++--+ state, and a Mulliken analysis of the net spin for the various magnetic and spin states of the Rh_2O_3(II) structural polymorph at 0 GPa.

	Energy (eV)	$\|\alpha-\beta\|$ Fe	$\|\alpha-\beta\|$ O average
AFM+−−++−−+	0	4.18	0.00
AFM++−−++−−	0.115	4.19	0.22
AFM++++−−−−	0.124	4.21	0.10
AFM+−+−+−+−	0.269	4.19	0.25
AFM+−+−−−++	0.155	4.20	0.15
AFM++−−−−++	0.119	4.22	0.03
FM	0.473	4.27	0.48
LS AFM+−−++−−+	1.706	1.06	0.01
LS FM	1.744	1.05	0.03

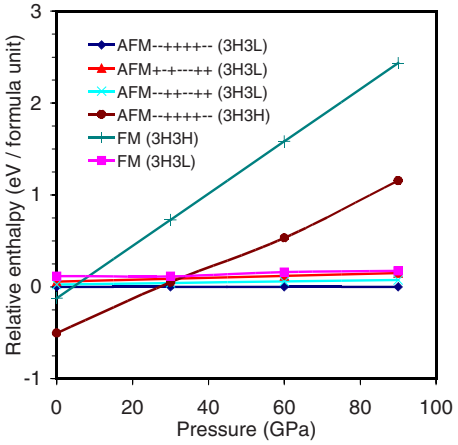

FIG. 8. (Color online) Enthalpies of the selected magnetic orderings considered for the distorted perovskite $GdFeO_3$ structured Fe_2O_3 plotted relative to AFM−−++++−− state.

mula unit less stable than the lowest-energy antiferromagnetic solution at 0 GPa (Table IV), and is computed to become increasingly less stable with increasing pressure. At 0 GPa the least stable solution considered is the ferromagnetic low-spin Fe state, which is computed to be 1.7 eV per formula unit less stable than the high-spin AFM+−−++−−+ state. Several antiferromagnetic arrangements with the low-spin Fe were tested and the lowest-energy solution was found with the +−−++−−+ ordering, and was computed to increase the stability of the low-spin state by 0.04 eV per formula unit. Relative to the high-spin AFM+−−++−−+ solution, the low-spin AFM+−−++−−+ solution becomes more stable with increasing pressure, and is calculated to be the most stable arrangement for Rh_2O_3(II) at pressures above 52 GPa.

Net spin of Fe calculated from a Mulliken population analysis (Table IV) gives values for the Rh_2O_3(II) polymorph, which are quite close to that calculated for the corundum structure, in both the high-spin and low-spin states. Under compression the change in the Rh_2O_3(II) structure is less anisotropic than in hematite. In hematite there is a 4% decrease in the **c**/**a** ratio between 0 and 90 GPa, while in the Rh_2O_3(II) structure the largest distortion between **a**, **b**, and **c**, is a 2% reduction in the **c**/**a** ratio.

C. Orthorhombic perovskite structure

The enthalpies of the various magnetic and spin states of perovskite structured Fe_2O_3 are plotted in Fig. 8. Unlike the corundum and Rh_2O_3(II) structures, orthorhombic perovskite has two distinct cation sites, which allows for the possibility of a mixed Fe^{2+}/Fe^{4+} charge state, or for the cations to have different spin states, i.e., one cation in a high-spin state and the other in a low spin. The enthalpies in Fig. 8 are plotted relative to the state with a high-spin Fe^{3+} in the eightfold site and a low-spin Fe^{3+} in the sixfold site (3H3L) and with the magnetic ordering AFM−−++++−−, as given by the atom labeling in Fig. 3.

For the perovskite structure the most stable electronic configurations were found with the cation in the 3+ state, with Fe^{2+}/Fe^{4+} solutions difficult to converge and much higher in energy. At 0 GPa the most stable arrangement calculated had both cations sites filled with high-spin Fe^{3+}, but at pressures above 26 GPa a more stable arrangement was found with a low-spin Fe^{3+} in the sixfold site, while the eightfold site remained high spin. The lowest-energy magnetic state found was with the ordering AFM−−++++−−, in which cations within (001) planes have alternating spin. When both cation sites contained high-spin Fe^{3+}, the AFM −−++++−− configuration was found to be 0.38 eV per formula unit more stable than the ferromagnetic arrangement, at 0 GPa. With increasing pressure the antiferromagnetic solution becomes increasingly more stable relative to the ferromagnetic solution, and at 90 GPa the energy difference is 1.28 eV per formula unit. With the mixed-spin (3H3L) configuration, the antiferromagnetic stabilization was computed to be smaller, with the AFM−−++++−− magnetic ordering being 0.12 eV per formula unit lower in energy than the ferromagnetic ordering.

Table V gives the relative stability of the electronic arrangements, and the net spin on atoms from a Mulliken population analysis. The values of 4.1 $|e|$ for high-spin Fe^{3+} and ~1 $|e|$ for low-spin Fe^{3+} are similar to the values computed for high- and low-spin Fe^{3+} in the other polymorphs.

D. $CaIrO_3$ structure

As in the perovskite case, there are two distinct cation sites in the $CaIrO_3$ structure (a sixfold and an eightfold), again allowing for a range of possible spin and charge combinations for iron. Enthalpies of the $CaIrO_3$-structured Fe_2O_3 in the various magnetic and spin states computed are shown in Fig. 9, with the magnetic states labeled from Fig. 4. Table VI details the relative stability of the different magnetic and spin arrangements at 60 GPa. At 60 GPa the most stable arrangement computed was with the larger eightfold cation site containing high-spin Fe^{3+} and the smaller sixfold cation site having low-spin Fe^{3+}, and antiferromagnetic coupling within the (010) layers (AFM+−+−). The enthalpies in Fig. 9 are plotted relative to this state.

TABLE V. Energies (eV per formula unit) relative to the AFM−−++++−− state, and a Mulliken analysis of the net spin for the various magnetic and spin states of the orthorhombic perovskite structural polymorph at 30 GPa

	Energy (eV)	$\lvert\alpha-\beta\rvert$ Fe in sixfold site	$\lvert\alpha-\beta\rvert$ Fe in eightfold site	$\lvert\alpha-\beta\rvert$ O
High-spin Fe in eightfold site and low-spin Fe in sixfold site				
FM	0.116	4.16	1.03	0.27
AFM−−++++−−	0.000	4.12	0.98	0.09
AFM++−−+−+−	0.072	4.14	0.98	0.07
AFM++−−++−−	0.042	4.14	0.97	0.07
AFM−−+++−−+	0.006	4.13	0.99	0.08
High spin Fe in eightfold site and high spin Fe in sixfold site				
FM	0.726			
AFM−−++++−−	0.050	4.13	4.12	0.08

As was found for the perovskite structure, at 0 GPa the most stable configuration computed was with both cations in a high-spin Fe^{3+} state, and for the $CaIrO_3$ structure, the lowest energy AFM+−+− ordering was computed to be 1.0 eV per formula unit more stable than the ferromagnetic solution at 0 GPa. In the mixed high-spin/low-spin configuration, the magnetic stabilization was much smaller, with the difference between the ferromagnetic and AFM+−+− solutions being 0.08 eV per formula unit at 60 GPa. The high-spin/low-spin Fe^{3+} solution is computed to be more stable than the high-spin/high-spin state at pressures above 37 GPa.

E. Relative stability of the polymorphs and their Néel temperatures

Calculated enthalpies of selected magnetic and spin states from the four polymorphs are plotted relative to the corundum high-spin AFM+−−+ state in Fig. 10. At 0 K both the orthorhombic perovskite and Rh_2O_3(II) polymorphs are calculated to only exist as metastable polymorphs, with the $CaIrO_3$ structure becoming the stable polymorph above 46 GPa.

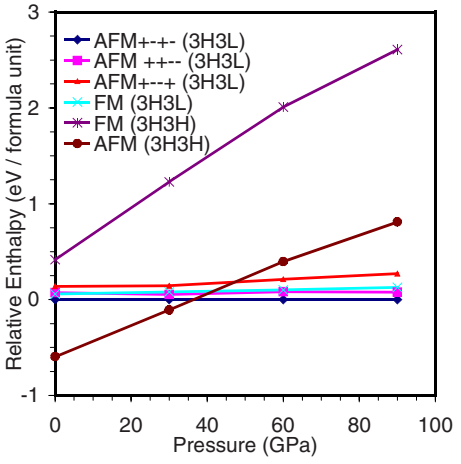

FIG. 9. (Color online) Enthalpies of the selected magnetic orderings considered for the $CaIrO_3$ structured Fe_2O_3 plotted relative to AFM+−+− state.

It has been proposed[1] from experiment that at low temperatures the orthorhombic perovskite structure is kinetically inhibited from forming so the Rh_2O_3(II) structure at 50 GPa is metastable with respect to the perovskite structure. Our results are consistent with this picture, and we calculate the corundum to Rh_2O_3(II) transition to occur at 47 GPa. However, the calculations do not agree with experiment on the high-temperature corundum to perovskite transition. The experimental results,[1] when extrapolated to 0 K, give a transition pressure between 23 and 27 GPa. As will be discussed in Sec. IV, the present calculations show the 0 K phase stability of the polymorphs, where they are below their respective Néel temperatures.

An estimate of the Néel temperature can be made by using a simple Ising Hamiltonian to compute the transition temperature within the mean-field approximation.[22] Although the simplicity of this Hamiltonian leads to only very approximate estimates of the transition temperature, it is still useful

TABLE VI. Energies (eV per formula unit) relative to the AFM+-+- state, and a Mulliken analysis of the net spin for the various magnetic and spin states of the $CaIrO_3$ structural polymorph at 60 GPa

	Energy (eV)	$\lvert\alpha-\beta\rvert$ Fe site 1	$\lvert\alpha-\beta\rvert$ Fe site 2
High-spin Fe in small cation site and low-spin Fe in the large cation site			
AFM+−+−	0	4.11	0.98
FM	0.080	4.13	1.08
AFM++−−	0.061	4.13	0.84
AFM+−−+	1.019	4.11	0.96
High-spin Fe in both large and small cation sites			
FM	1.987		
AFM+−+−	0.375		

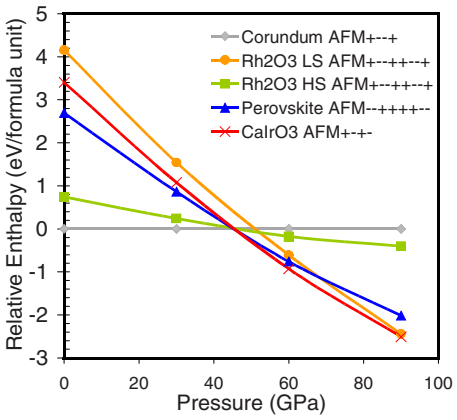

FIG. 10. (Color online) Selected enthalpies of the four polymorphs of Fe_2O_3, plotted relative to the corundum AFM+−−+ state.

for a qualitative comparison of the magnetic transition temperatures of the various structural polymorphs. At 0 GPa we calculate the Néel temperature of hematite to be 1040 K, compared with the experimental value of 948 K.[14] This value is lower than the value of 1711 K (Ref. 22) calculated within the LDA, reflecting the lower-energy differences between the magnetic states calculated within the B3LYP approximation.

Using the same approach as above, we calculate an approximate Néel temperature for the Rh_2O_3(II) structure of 1270 K. For the perovskite polymorph, the energy differences between the magnetic states are smaller than those for the corundum and Rh_2O_3(II) structures, and consequently, the calculated Néel temperature for this structure is lower, at 340 K.

IV. DISCUSSION

The magnetic properties of the four structural polymorphs play an important role in determining their phase stability, and with increasing pressure there is a general trend for a greater stabilization of the antiferromagnetic phase. In hematite an important contribution to the stabilization of the antiferromagnetic solution is the electron superexchange mechanism,[33,54] whereby stabilization is found by the antiferromagnetic coupling of the net spin moments of two Fe atoms through the electron distribution of an in-between O atom. Superexchange interactions can be classified into σ-type and π-type superexchange, with the σ-type superexchange being stronger and at its greatest through metal-oxygen-metal bond angles of 180°, weakening as the angle approaches 90°. In high-spin Fe^{3+} the d^5 configuration having half-filled e_g orbitals leads to strong sigma type cation-anion-cation interactions. In the corundum structure the lowest-energy magnetic ordering at 0 GPa is calculated to be AFM+−−+, where the antiferromagnetic coupling takes place through Fe-O-Fe bond angles of 132° (x 6), 119° (x 3), and 86° (x 1). The antiferromagnetic coupling in the AFM ++−− ordering, which is 0.25 eV per formula unit less stable than the AFM+−−+ ordering, takes place through Fe-O-Fe bond angles of 132° (x 6) and 94° (x 3), and the AFM+−+− ordering, 0.32 eV per formula unit less stable than the AFM+−−+ ordering, takes place through bond angles of 119° (x 3), 94° (x 3), and 86° (x 1). This ordering is different than that computed within the GGA (Ref. 21) and LDA (Ref. 22) formalisms, where the AFM+−+− was found to be lower in energy than the AFM++−−, but is the same as the ordering found using HF.[39]

In the Rh_2O_3(II) structure the largest Fe-O-Fe bond angle is 130° found for bonds with two Fe cations in the same (001) plane. Of all the antiferromagnetic solutions considered for the Rh_2O_3(II) structure, the three least stable have ferromagnetic ordering within (001) planes. In the orthorhombic perovskite structure there are both high-spin and low-spin Fe^{3+} cations. The largest Fe-O-Fe bond angle in this structure is 152° found between high-spin Fe cations in the (110) plane. The most stable antiferromagnetic orderings are found with antiferromagnetic coupling though this bond.

The results show that the B3LYP functional provides a good description of the properties of bulk hematite, such as the cell parameters, bulk modulus, and magnetic ordering. Rollman *et al.*[21] showed that the GGA predicts a collapse of the magnetic moment, from the HS antiferromagnetic solution to a LS ferromagnetic solution at 14 GPa, a result that is inconsistent with experiment. Experimentally, no HS to LS transition is observed in the corundum structure, and by using a DFT+U method, Rollman *et al.*[21] showed that this HS to LS transition was no longer predicted to occur for values of $U \geq 4$. Using the B3LYP functional we find that for the corundum structure, the HS AFM+−−+ solution collapses to a LS AFM+−−+ solution at 56 GPa, a result which is not inconsistent with experiment, as at this pressure the corundum structure is no longer the stable polymorph.

Ono *et al.*[1] proposed that the transition seen at about 50 GPa in room-temperature experiments be attributed to a transformation from a corundum to a metastable Rh_2O_3(II) structure, with the lower-energy perovskite structure being kinetically inhibited from forming and so only obtainable at higher temperatures. In comparing our results to experiment, we note that at room temperature the transition is taking place below the experimental Néel temperature of hematite and our estimated Néel temperature of the Rh_2O_3(II) structure.

Figure 10 shows that our calculations also predict the Rh_2O_3(II) structure to be metastable with respect to the perovskite structure at 50 GPa. We compute that the high-spin antiferromagnetic Rh_2O_3(II) structure becomes more stable than the high-spin antiferromagnetic corundum structure at 47 GPa, with a spin crossover to a low-spin antiferromagnetic Rh_2O_3(II) solution calculated to occur at 52 GPa. These transition pressures are in good agreement with the experimental values given in Badro *et al.*[8] In that experiment hematite was compressed to 46 GPa, at which it showed no crystallographic or spin change, then slightly heated, enough to nucleate the Rh_2O_3(II) phase but not another high-pressure phase. The Rh_2O_3(II) phase was found to have Fe in a low-spin state. After relaxing at 46 GPa for ten hours the phase remained in a Rh_2O_3(II) structure, but the Fe reverted to a high-spin state. The calculations presented in Fig. 10 are in agreement with this experiment with the closeness in pressure of the calculated corundum high spin to Rh_2O_3(II) high spin transition and the calculated Rh_2O_3(II) high spin to

Rh_2O_3(II) low spin transition. The transition to low-spin Fe is not required to obtain the high-pressure phase. This agreement with experiment suggests that in this case the B3LYP functional is accurately modeling the HS to LS transition in the Fe.

In high-temperature experiments (>1000 K) Fe_2O_3 is found to undergo a phase transformation from the corundum structure at about 30 GPa. Ono *et al.*[1] experimentally determined the transition boundary to be represented by the equation

$$P(\text{GPa}) = 29.4(\pm 0.4) + 0.0046(\pm 0.0015) \times [T(\text{K}) - 1000] \quad (1)$$

and attributed the transition as a corundum to perovskite transformation. When extrapolated to 0 K, Eq. (1) gives a phase transition of between 23 and 27 GPa. Our calculated enthalpies shown in Fig. 10 give the corundum to perovskite transition pressure of about 47 GPa, significantly higher than the extrapolated experimental value. We believe an explanation for this discrepancy may be the following.

To overcome kinetic effects, high temperatures are often required for phase transitions to occur. However in the case of hematite, with a Néel temperature of 948 K, heating to over 1000 K also changes the magnetic structure of the material, from antiferromagnetic at 0 K to being paramagnetic above the Néel temperature. Extrapolation from the high-temperature experiments does not consider the change in internal energy between the paramagnetic and antiferromagnetic states. With the larger magnetic stabilization of the corundum phase, there is likely to be a greater destabilization in the internal energy of the corundum phase compared to the orthorhombic perovskite in going from the antiferromagnetic solution to the paramagnetic solution. This would have the effect of lowering the transition pressure from our calculated antiferromagnetic solutions, suggesting that in addition to overcoming possible kinetic effects, the high temperature required for the 30 GPa transition is also needed to change the magnetic state of hematite.

Experimentally, the $CaIrO_3$-type structure is found to occur at pressures above 60 GPa and temperatures greater than 1200 K,[3] and when extrapolated to 0 K the transition pressure is estimated to be between 50 and 63 GPa. Once again care must be taken in extrapolating the high-temperature experiments to 0 K, as the magnetic state in the high-temperature experiments is not the same as that of the 0 K calculations. The (>1200 K) temperatures required to drive the transformation are above the estimated Néel temperatures of both the perovskite and $CaIrO_3$ polymorphs. Our calculations predict stability of the $CaIrO_3$ structure with respect to the perovskite structure at 46 GPa at 0 K. That the calculated pressure is close to the 0 K extrapolated value is possibly due to the smaller and similar magnetic energies of the perovskite and $CaIrO_3$ phase.

V. CONCLUSIONS

This study of Fe_2O_3 has shown that the results of hybrid B3LYP calculations are in very good agreement with experiment in predicting the structural, elastic, electronic, and magnetic properties of hematite. For all of the structural polymorphs of Fe_2O_3 considered here, the most stable configurations found were with Fe^{3+}. In the orthorhombic perovskite and $CaIrO_3$-type structures we did not find an Fe^{2+}/Fe^{4+} solution stable, rather, both structures took a mixed high-spin low-spin Fe^{3+} configuration at high pressures. For the corundum structure the B3LYP calculations predict an antiferromagnetic ordering that is in agreement with experiment. We find antiferromagnetic orderings also give the lowest-energy solutions for the other structural polymorphs, and that consideration of magnetic properties is important to understanding of the stability of the high-pressure phases. The calculations are in agreement with the low-temperature transition found experimentally at 50 GPa, predicting it to be a corundum to Rh_2O_3(II) transformation, however the calculations do not predict the high-temperature transition that occurs at 30 GPa.

ACKNOWLEDGMENTS

The authors wish to acknowledge the support of the Australian partnership for Advanced Computing (APAC) and the Victorian Partnership for Advanced Computing (VPAC) supercomputer facilities. The authors thank Ian Grey and Graham Sparrow for their useful comments.

[1] S. Ono, K. Funakoshi, Y. Ohishi, and E. Takahashi, J. Phys.: Condens. Matter **17**, 269 (2005).
[2] S. Ono, T. Kikegawa, and Y. Ohishi, J. Phys. Chem. Solids **65**, 1527 (2004).
[3] S. Ono and Y. Ohishi, J. Phys. Chem. Solids **66**, 1714 (2005).
[4] H. Liu, W. A. Caldwell, L. R. Benedetti, W. Panero, and R. Jeanloz, Phys. Chem. Miner. **30**, 582 (2003).
[5] M. P. Pasternak, G. K. Rozenberg, G. Y. Machavariani, O. Naaman, R. D. Taylor, and R. Jeanloz, Phys. Rev. Lett. **82**, 4663 (1999).
[6] G. K. Rozenberg, L. S. Dubrovinsky, M. P. Pasternak, O. Naaman, T. Le Bihan, and R. Ahuja, Phys. Rev. B **65**, 064112 (2002).
[7] S. H. Shim and T. S. Duffy, Am. Mineral. **87**, 318 (2002).
[8] J. Badro, G. Fiquet, V. V. Struzhkin, M. Somayazulu, H.-k. Mao, G. Shen, and T. Le Bihan, Phys. Rev. Lett. **89**, 205504 (2002).
[9] J. S. Olsen, C. S. G. Cousins, L. Gerward, H. Jhans, and B. J. Sheldon, Phys. Scr. **43**, 327 (1991).
[10] Y. Syono, A. Ito, S. Morimoto, T. Suzuki, T. Yagi, and S. Akimoto, Solid State Commun. **50**, 97 (1984).
[11] I. de P. R. Moreira, F. Illas, and R. L. Martin, Phys. Rev. B **65**, 155102 (2002).
[12] L. Pauling and S. B. Hendricks, J. Am. Chem. Soc. **47**, 781 (1925).

[13] A. Fujimori, M. Saeki, N. Kimizuka, M. Taniguchi, and S. Suga, Phys. Rev. B **34**, 7318 (1986).
[14] A. H. Morrish, *Canted Antiferromagnetism, Hematite* (World Scientific, Singapore, 1994).
[15] C. G. Shull, W. A. Strauser, and E. O. Wollan, Phys. Rev. **83**, 333 (1951).
[16] N. Amin and S. Arajs, Phys. Rev. B **35**, 4810 (1987).
[17] M. Murakami, K. Hirose, K. Kawamura, N. Sata, and Y. Ohishi, Science **304**, 855 (2004).
[18] A. R. Oganov and S. Ono, Nature (London) **430**, 445 (2004).
[19] K. Hirose, K. Kawamura, Y. Ohishi, S. Tateno, and N. Sata, Am. Mineral. **90**, 262 (2005).
[20] J. Tsuchiya, T. Tsuchiya, and R. M. Wentzcovitch, Phys. Rev. B **72**, 020103(R) (2005).
[21] G. Rollmann, A. Rohrbach, P. Entel, and J. Hafner, Phys. Rev. B **69**, 165107 (2004).
[22] L. M. Sandratskii, M. Uhl, and J. Kubler, J. Phys.: Condens. Matter **8**, 983 (1996).
[23] V. R. Saunders, R. Dovesi, C. Roetti, R. Orlando, C. M. Zicovich-Wilson, N. M. Harrison, K. Doll, B. Civalleri, I. J. Bush, Ph. D'Arco, and M. Llunell, *CRYSTAL2003 User's Manual* (University of Torino, Torino, 2003).
[24] A. D. Becke, J. Chem. Phys. **98**, 5648 (1993).
[25] X. B. Feng and N. M. Harrison, Phys. Rev. B **69**, 132502 (2004).
[26] X. B. Feng and N. M. Harrison, Phys. Rev. B **69**, 035114 (2004).
[27] D. Munoz, N. M. Harrison, and F. Illas, Phys. Rev. B **69**, 085115 (2004).
[28] J. Muscat, A. Wander, and N. M. Harrison, Chem. Phys. Lett. **342**, 397 (2001).
[29] N. C. Wilson, J. Muscat, D. Mkhonto, P. E. Ngoepe, and N. M. Harrison, Phys. Rev. B **71**, 075202 (2005).
[30] N. C. Wilson, S. P. Russo, J. Muscat, and N. M. Harrison, Phys. Rev. B **72**, 024110 (2005).
[31] R. L. Martin and F. Illas, Phys. Rev. Lett. **79**, 1539 (1997).
[32] J. D. Pack and H. J. Monkhorst, Phys. Rev. B **16**, 1748 (1977).
[33] M. Catti, G. Valerio, and R. Dovesi, Phys. Rev. B **51**, 7441 (1995).
[34] K. Doll, V. R. Saunders, and N. M. Harrison, Int. J. Quantum Chem. **82**, 1 (2001).
[35] B. Civalleri, P. D'Arco, R. Orlando, V. R. Saunders, and R. Dovesi, Chem. Phys. Lett. **348**, 131 (2001).
[36] S. Mochizuki, Phys. Status Solidi A **41**, 591 (1977).
[37] J. K. Leland and A. J. Bard, J. Phys. Chem. **91**, 5076 (1987).
[38] M. P. J. Punkkinen, K. Kokko, W. Hergert, and I. J. Vayrynen, J. Phys.: Condens. Matter **11**, 2341 (1999).
[39] M. Catti and G. Sandrone, Faraday Discuss. **106**, 189 (1997).
[40] T. Droubay, K. M. Rosso, S. M. Heald, D. E. McCready, C. M. Wang, and S. A. Chambers, Phys. Rev. B **75**, 104412 (2007).
[41] A. Bandyopadhyay, J. Velev, W. H. Butler, S. K. Sarker, and O. Bengone, Phys. Rev. B **69**, 174429 (2004).
[42] J. Velev, A. Bandyopadhyay, W. H. Butler, and S. Sarker, Phys. Rev. B **71**, 205208 (2005).
[43] V. I. Anisimov, J. Zaanen, and O. K. Andersen, Phys. Rev. B **44**, 943 (1991).
[44] G. Dräger, W. Czolbe, and J. A. Leiro, Phys. Rev. B **45**, 8283 (1992).
[45] C. Y. Kim, M. J. Bedzyk, E. J. Nelson, J. C. Woicik, and L. E. Berman, Phys. Rev. B **66**, 085115 (2002).
[46] R. Sato and S. Akimoto, J. Appl. Phys. **50**, 5285 (1979).
[47] D. R. Wilburn and W. A. Basset, J. Geophys. Res. **83**, 3509 (1978).
[48] R. C. Liebermann and E. Schreiber, J. Geophys. Res. **73**, 6585 (1968).
[49] L. W. Finger and R. M. Hazen, J. Appl. Phys. **51**, 5362 (1980).
[50] F. D. Murnaghan, Proc. Natl. Acad. Sci. U.S.A. **30**, 244 (1944).
[51] I. P. R. Moreira and F. Illas, Phys. Chem. Chem. Phys. **8**, 1645 (2006).
[52] G. S. E. J. Samuelsen, Phys. Status Solidi **42**, 241 (1970).
[53] X. B. Feng and N. M. Harrison, Phys. Rev. B **70**, 092402 (2004).
[54] J. B. Goodenough, *Magnetism and the Chemical Bond* (Interscience, New York, 1963).